The Astrophysical Journal, 656:483–492, 2007 February 10

COMPUTING LIMB-DARKENING COEFFICIENTS FROM STELLAR ATMOSPHERE MODELS

David Heyrovský
Institute of Theoretical Physics, Charles University, Prague, Czech Republic; david.heyrovsky@mff.cuni.cz
Received 2005 December 21; accepted 2006 September 18

ABSTRACT

We explore the sensitivity of limb-darkening coefficients computed from stellar atmosphere models to different least-squares fitting methods. We demonstrate that conventional methods are strongly biased to fitting the stellar limb. Our suggested method of fitting by minimizing the radially integrated squared residual yields improved fits with better flux conservation. The differences of the obtained coefficients from commonly used values are observationally significant. We show that the new values are in better agreement with solar limb-darkening measurements, as well as with coefficients reported from analyses of eclipsing binary light curves.

Subject headings: binaries: eclipsing — methods: numerical — stars: atmospheres

1. INTRODUCTION

With the exception of our Sun, up to recently the observational significance of stellar limb darkening had been limited to the analysis of eclipsing binary light curves (Popper 1984). A range of new observational techniques and strategies sensitive to limb darkening has been developed since then. These include, for example, stellar surface interferometry (Quirrenbach et al. 1996), observation of gravitational microlensing caustic-crossing events (Witt 1995), and extrasolar planet transits (Deeg et al. 2001). When analyzing any such measurements, expected intensity profiles from stellar atmosphere models are often used in the process of determining other event parameters. However, with sufficiently good quality data these observations can also be used for direct measurements of stellar limb darkening.

Such measurements are usually done by assuming simple analytical limb-darkening laws. The measured coefficients of these laws are then compared with their theoretically predicted values, which are obtained by fitting the laws to model atmosphere intensity profiles. However, these predicted values depend significantly on the adopted method of fitting (e.g., Díaz-Cordovés et al. 1995). Here we demonstrate that even variants of the commonly used least-squares methods can yield very different coefficient values, and we suggest a preferred method of fitting.

In the following section, § 2, we discuss various fitting methods and introduce our suggested method. We study the fit qualities of selected methods in § 3 and demonstrate the differences between obtained coefficients on the example of ATLAS model atmospheres (Kurucz 1993a). In § 4.1 we compare these coefficients with measured solar limb darkening, and in § 4.2 we compare them with limb-darkening coefficient estimates available from eclipsing binary light-curve analyses. We discuss variations of the suggested fitting method in § 5 and summarize the main conclusions in § 6.

2. LIMB-DARKENING LAW FITTING METHODS

One of the main results obtained from stellar atmosphere models is the center-to-limb variation of specific intensity I_ν of the emitted radiation field, computed for a range of wavelengths. The center-to-limb dependence is obtained by computing radiative transfer along a set of rays emerging from the atmosphere under different viewing angles θ. Broadband limb darkening of the intensity I can then be computed from I_ν for different photometric filter systems. Intensity values are traditionally parameterized by $\mu = \cos\theta$, ranging from 1 at the stellar disk center to 0 at the limb, or alternatively by the radial position on the disk, $r = \sin\theta$, ranging from 0 at the center to 1 at the limb.

Various analytical laws have been suggested for approximating stellar limb darkening, most of them in the form of linear combinations of simple functions of μ. The most basic limb-darkening law, generally referred to as "linear limb darkening," is given by

$$I_L(\mu) = I_0[1 - u(1 - \mu)], \tag{1}$$

where the linear limb-darkening coefficient u determines the shape of the limb-darkening profile and I_0 is the intensity of the linear law at the disk center. Other laws have been introduced to get a more accurate analytical description by adding a third term to equation (1), such as the quadratic, square root, or logarithmic laws (see Claret 2000). Claret (2000) also proposed a more complex law that is a linear combination of five terms.

2.1. *Previous Fitting Methods*

A range of methods have been used for the seemingly straightforward task of computing limb-darkening coefficients from the intensity profiles of model atmospheres, each of them producing generally different values. The two main groups of fitting methods are least-squares–based methods (e.g., Manduca et al. 1977; Claret & Giménez 1990; Díaz-Cordovés et al. 1995; Claret et al. 1995) and methods requiring flux conservation (e.g., Wade & Rucinski 1985; Van Hamme 1993). The primary motivation for the latter methods is the observation that by concentrating on the quality of the fit of the profile shape, one often ends up with a low accuracy of flux conservation. This problem is especially pronounced in the case of the linear law, less so in higher order laws. Computation of higher order coefficients in the flux-conservation methods requires additional constraints; for example, conservation of mean intensity (Van Hamme 1993), or fixing the intensity value at $\mu = 0.1$ close to the limb (Wade & Rucinski 1985).

Least-squares–based methods compute limb-darkening coefficients mostly by minimizing

$$\chi^2 = \sum_i [I_L(\mu_i) - I_i]^2, \tag{2}$$

where I_i is the intensity of the model atmosphere at disk position μ_i and I_L is the limb-darkening law of interest. In support of the least-squares methods, Claret (2000) argues that flux-conservation

methods fail in the main reason for using analytical laws, which is to get a reasonable fit of the shape of the intensity profile. A good fit to the profile, particularly in the case of higher order laws, should inherently lead to sufficiently accurate flux conservation. In comparison, by concentrating on integrated quantities, flux-conservation methods largely ignore the shape of the profile.

We note here that in earlier works based on either of the methods (e.g., all those cited in the first paragraph of this subsection), the central intensity I_0 was kept fixed at the model atmosphere value, and only the shape-defining limb-darkening coefficients were fitted. However, there is no a priori reason to fix one particular point in the intensity profile at its exact value and fit only the remaining points. On the other hand, this approach leads to an overall worse fit. In more recent works, this constraint has been apparently dropped (Claret 2000; Barban et al. 2003). In the case of the linear law from equation (1), the simplest approach is to fit the linear parameters I_0 and uI_0 and compute the limb-darkening coefficient u as the ratio of the obtained values. All the other laws mentioned above can be fitted in a similar manner.

The least-squares method has its own further ambiguities. As pointed out by Díaz-Cordovés et al. (1995), the obtained coefficients depend on the distribution of the rays μ_i provided by the model atmospheres. For example, in the commonly used Kurucz ATLAS9 models (Kurucz 1993a, 1993b, 1993c, 1994), the spacing of the 17 computed rays decreases sharply at low values of μ, close to the limb. A straightforward fit minimizing equation (2) then gives a high weight to the quality of the fit close to the limb on account of the fit quality closer to the center. In order to get a less biased fit, Díaz-Cordovés et al. (1995), as well as subsequently Claret et al. (1995) and Claret (2000), used only a subset of the available rays that were more evenly spaced in μ. Similarly, Barban et al. (2003), who used their own ATLAS-based model atmospheres, computed 20 rays evenly distributed in μ.

2.2. *Suggested Fitting Method*

A simple way to overcome problems caused by the spacing of discrete points $[\mu_i, I_i]$ is to suitably interpolate the intensity between the points so that we get a continuous function $\tilde{I}(\mu)$ that passes through all the model points, $\tilde{I}(\mu_i) = I_i$. For this purpose we can use cubic spline interpolation. The I_i versus μ_i dependence is typically smooth, without large jumps or wiggles, so such a spline gives a reasonable interpolation. The limb-darkening coefficients can now be computed by minimizing the integrated squared residual

$$\Delta_\mu^2 = \int \left(I_L - \tilde{I}\right)^2 d\mu, \tag{3}$$

where all integrals appearing in the least-squares solution can be evaluated to arbitrary precision. The result obtained in this way is what previous authors were trying to achieve by selecting regularly spaced points. In the suggested approach none of the points obtained from the model atmosphere computations are omitted, and thus no useful information is neglected. The spline interpolation provides a sensible guess about the behavior of the intensity in between these points. We discuss the sensitivity of the results to the particular choice of spline interpolation in § 5.

However, the ambiguity due to the spacing of points is only seemingly overcome. The new ambiguity lies in the choice of the integration variable in equation (3). In this example, integration over μ gives equal weight to the squared residual in equal-sized intervals of μ. For instance, the squared residual in the radial interval from the center to $r = 0.87$ (corresponding to $\mu = 0.5$) has the same weight as in the remaining interval close to the limb. By transforming from μ to the radial coordinate r in the integral in equation (3), we get

$$\Delta_\mu^2 = \int \left(I_L - \tilde{I}\right)^2 r\left(1 - r^2\right)^{-1/2} dr. \tag{4}$$

We see that the residual at the disk center has zero weight and the weight function grows monotonously toward the limb, where it diverges. The choice of μ as the integration variable thus still gives results that are strongly biased to fitting the limb of the star. In order to get a reasonable fit even closer to the center, we decided to integrate over r and compute limb-darkening coefficients by minimizing

$$\Delta_r^2 = \int \left(I_L - \tilde{I}\right)^2 dr. \tag{5}$$

The suitability of the choice of integration variable (or, equivalently, weighting) should be primarily demonstrated in confrontation with observational data, and we do so in § 4. In support of our choice, we briefly consider here some relevant astrophysical situations, namely, eclipsing binaries and caustic-crossing microlensing events. In both of these cases the weighting kernel that is convolved with the intensity to obtain the flux is time-dependent, depending on the phase of the binary or the position of the passing lens, respectively. Hence, neither scenario directly provides a single ideal weighting. However, if we look, for simplicity, at the case of a 90° inclination binary, the radial position of the occulting component shifts linearly with time. Moreover, for example, in the case of annular eclipses, the occulted area is of constant radial size. Similarly, in zero impact parameter single-lens microlensing, the radial position of the lens changes linearly with time, giving maximum weight at each position to the point directly behind the lens. Such considerations suggest that equal radial weighting is a natural and reasonable choice.

In the following section we illustrate the differences between the results obtained by the discussed fitting methods on the example of widely used model atmospheres.

3. DEMONSTRATION ON ATLAS ATMOSPHERES

We demonstrate the different fitting methods on the ATLAS9 model atmospheres computed by Kurucz (1993a, 1993b, 1993c, 1994) using the intensity files available on R. Kurucz's Web site.[1] The models in the parameter grid have metallicities ranging from $[\mathrm{Fe/H}] = +1$ to -5, effective temperatures from $T_{\mathrm{eff}} = 3500$ to 50,000 K, surface gravities in cgs units from $\log g = 0$ to 5, and microturbulent velocities for solar metallicity models from $v_t = 0$ to 8 km s^{-1}; for other metallicities, only $v_t = 2$ km s^{-1}. For each model, the specific intensity I_ν is given for wavelengths from $\lambda = 9.09$ nm to 160 μm, spaced by 2 nm in the optical range, and for 17 rays passing through the atmosphere: 10 rays at μ-values from 1 to 0.1, spaced by 0.1, and 7 additional rays close to the limb at 0.25, 0.15, 0.125, 0.075, 0.05, 0.025, and 0.01 (see Fig. 1). We obtain intensity profiles for specific photometric filters by integrating

$$I_i(\mu_i) = \int \frac{c}{\lambda^2} I_\nu(\mu_i, \lambda) S(\lambda)\, d\lambda, \tag{6}$$

where c/λ^2 is the specific intensity conversion factor (from per frequency to per wavelength) and $S(\lambda)$ is the filter response function.

[1] See http://kurucz.harvard.edu.

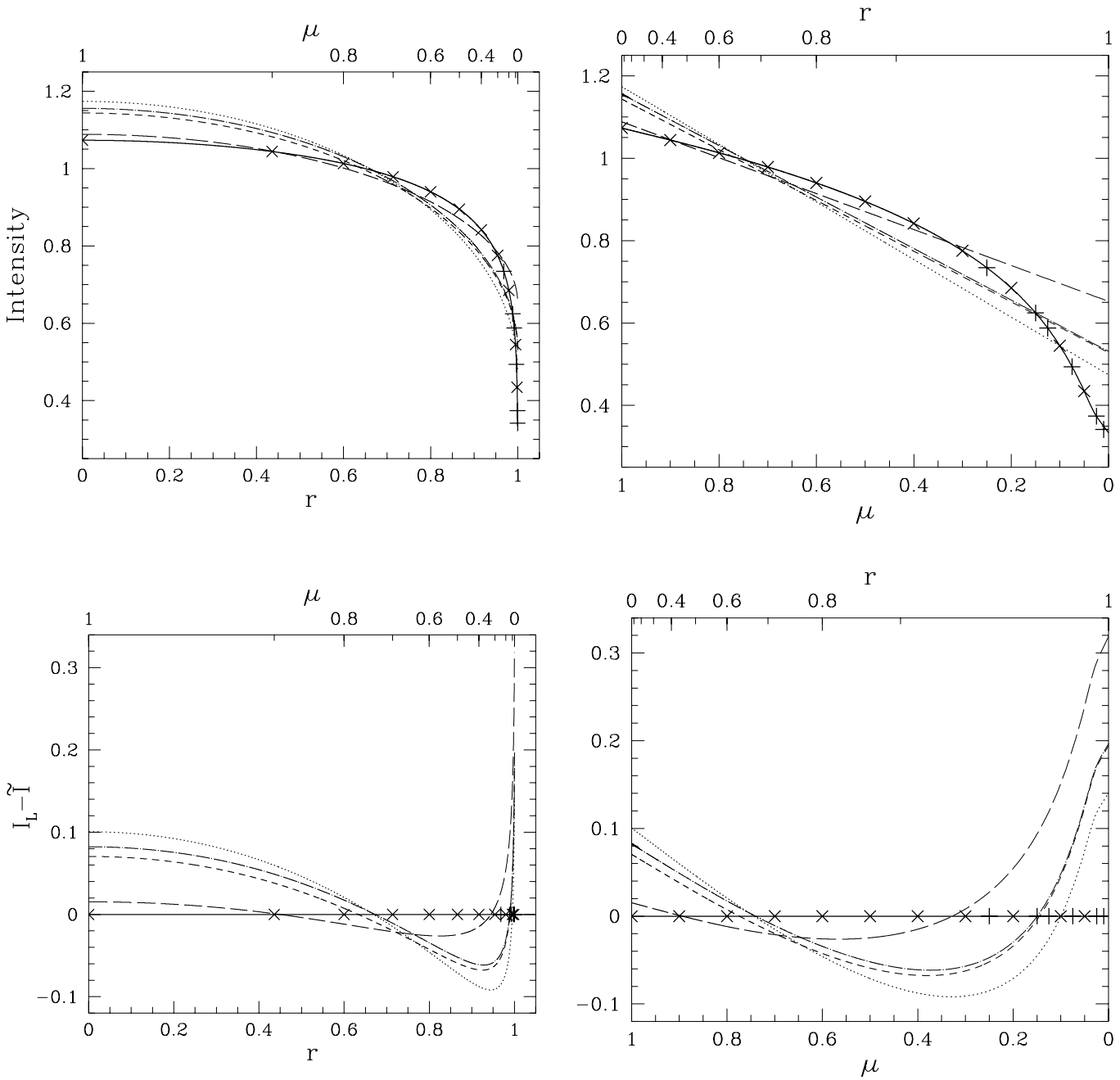

FIG. 1.— Sample Kurucz ATLAS9 model intensity profile ($T_{\rm eff} = 4250$ K, $\log g = 4.5$, [Fe/H] $= -3.5$, V band) and its different linear limb-darkening fits. The original 17 points are marked by crosses (11 points) and plus signs. Line types include the interpolated profile $\tilde{I}$ (*thick solid*), the 17-point fit (*dotted*; linear coefficient $u_{17} = 0.596$), the 11-point fit (*short-dashed*; $u_{11} = 0.538$), a fit of the interpolated $\tilde{I}$ by μ-integration (*dot-dashed*; $u_\mu = 0.540$), and a fit of $\tilde{I}$ by r-integration (*long-dashed*; $u_r = 0.401$). Intensity is shown in the top panels, and absolute residuals of fits from $\tilde{I}$ are shown in the bottom panels. The left panels are plotted as a function of r and the right panels are plotted as a function of μ, with respective alternate parameters marked along the upper axes.

In this work we use the standard *BVRI* filter response functions given by Bessell (1990). We formally extend the intensity profile to $\mu = 0$ by linear extrapolation from the two points closest to the limb and obtain $\tilde{I}(\mu)$ by interpolating the profile using cubic splines with natural boundary conditions. We discuss the influence of different boundary conditions in § 5.

We compare four different least-squares fitting methods. First, we fit all 17 points provided by Kurucz's models, minimizing the χ^2 given by equation (2). Second, we use the same equation to fit a subset of 11 points with 10 regularly spaced μ-values from 1 to 0.1, plus $\mu = 0.05$; these are the points fitted by Díaz-Cordovés et al. (1995), Claret et al. (1995), and Claret (2000). Third, we fit the spline-interpolated intensity $\tilde{I}$, minimizing Δ^2_μ from equation (3) and using integration over μ. Fourth is our suggested method, that of fitting $\tilde{I}$ by minimizing Δ^2_r from equation (5) and using integration over r.

In Figure 1 we present as an example the V-band profile of a $T_{\rm eff} = 4250$ K, $\log g = 4.5$, [Fe/H] $= -3.5$ model atmosphere, plotted separately as a function of r and μ. The plots include the original points and their spline-interpolated intensity profile $\tilde{I}$ (here normalized to unit r-integrated rms intensity), as well as linear limb-darkening laws fitted by the four methods and their residuals from $\tilde{I}$. As expected and as pointed out by Díaz-Cordovés et al. (1995), the 17-point fit has the heaviest bias to the limb. The 11-point fit here closely approximates the μ-integrated fit that has the lowest μ-integrated squared residual (see Fig. 1,

TABLE 1
Limb-darkening Fit Quality for Different Least-Squares Fitting Methods

LD Law	Method	Average σ (%)	Max. σ (%)	Average $\lvert\Delta F/F\rvert$	Max. $\lvert\Delta F/F\rvert$
Linear	17-point	3.327	6.987	3.63×10^{-3}	1.42×10^{-2}
	11-point	2.344	5.554	4.38×10^{-3}	1.29×10^{-2}
	μ-int. spline	2.706	6.275	1.18×10^{-16}	5.96×10^{-16}
	r-int. spline	1.253	3.527	2.27×10^{-3}	8.65×10^{-3}
Quadratic	17-point	1.180	3.303	3.85×10^{-3}	1.07×10^{-2}
	11-point	0.653	1.785	1.10×10^{-3}	2.98×10^{-3}
	μ-int. spline	0.980	2.609	6.38×10^{-16}	1.75×10^{-15}
	r-int. spline	0.417	0.991	2.35×10^{-4}	6.15×10^{-4}
Square root	17-point	0.498	3.545	1.13×10^{-3}	1.08×10^{-2}
	11-point	0.288	2.115	3.32×10^{-4}	4.71×10^{-3}
	μ-int. spline	0.415	3.256	4.21×10^{-16}	1.65×10^{-15}
	r-int. spline	0.238	1.382	1.28×10^{-4}	1.99×10^{-3}
Logarithmic	17-point	0.665	2.657	1.85×10^{-3}	8.70×10^{-3}
	11-point	0.345	1.587	5.35×10^{-4}	3.41×10^{-3}
	μ-int. spline	0.528	2.363	1.85×10^{-16}	7.91×10^{-16}
	r-int. spline	0.259	0.999	1.66×10^{-4}	1.18×10^{-3}
Claret	17-point	0.190	0.625	8.27×10^{-5}	5.05×10^{-4}
	11-point	0.175	0.558	4.57×10^{-5}	2.17×10^{-4}
	μ-int. spline	0.184	0.585	4.48×10^{-16}	2.62×10^{-15}
	r-int. spline	0.170	0.550	1.81×10^{-5}	5.48×10^{-5}

Note.—Average and maximum values of the relative rms residual σ and the relative flux excess $\lvert\Delta F/F\rvert$, evaluated for *BVRI* profiles of the full range of Kurucz model atmospheres (see text).

bottom right), and both are only slightly less biased to the limb. The *r*-integrated fit by definition has the lowest *r*-integrated squared residual (see Fig. 1, *bottom left*). The non-integrated residuals of this fit are overall the smallest from the center to roughly $\mu = 0.2$ (i.e., $r = 0.98$). Although the quality of the μ-integrated fit is substantially better on the remaining interval, the radial width of this interval is only 0.02. We conclude that the *r*-integrated fit gives the best linear limb-darkening approximation of the intensity profile.

In order to compare the fitting methods more generally, we fitted *BVRI* profiles of the full range of models described above, a set comprising 38,324 profiles of 9581 model atmospheres altogether. Besides the linear law, we used quadratic, square root, logarithmic, and Claret limb-darkening laws (for definitions, see Claret 2000). For each fit we computed two parameters as measures of fit quality. The first is the relative rms residual, defined as the ratio of the rms residual to the rms intensity,

$$\sigma = \frac{\Delta_r}{\sqrt{\int \tilde{I}^2\, dr}}. \tag{7}$$

Our second parameter is the relative flux excess of the obtained fit over the original profile,

$$\frac{\Delta F}{F} = \frac{\int I_L r\, dr}{\int \tilde{I} r\, dr} - 1. \tag{8}$$

The average and maximum absolute values of these parameters for the five limb-darkening laws and four fitting methods are presented in Table 1. Judging by the residuals σ, for all the laws *r*-integration by definition gives the best results (for the linear law, the average $\sigma = 1.25\%$; the worst fitted profile has $\sigma = 3.53\%$), followed by the substantially worse 11-point fit (2.34%, 5.55%), μ-integration (2.71%, 6.28%), and the poorest 17-point fit (3.33%, 6.99%).

Comparing the fitting methods by relative flux excess yields a different picture. For all the laws μ-integration gives by far the best flux conservation (here limited by machine precision; for the linear law, the formal average of $\lvert\Delta F/F\rvert = 1.18 \times 10^{-16}$; the highest value for a profile of $\lvert\Delta F/F\rvert = 5.96 \times 10^{-16}$), followed by *r*-integration (2.27×10^{-3}, 8.65×10^{-3}). Except in the case of the linear law, where the order of the remaining methods is reversed, these are followed by the 11-point fit (4.38×10^{-3}, 1.29×10^{-2}) and the 17-point fit (3.63×10^{-3}, 1.42×10^{-2}). The

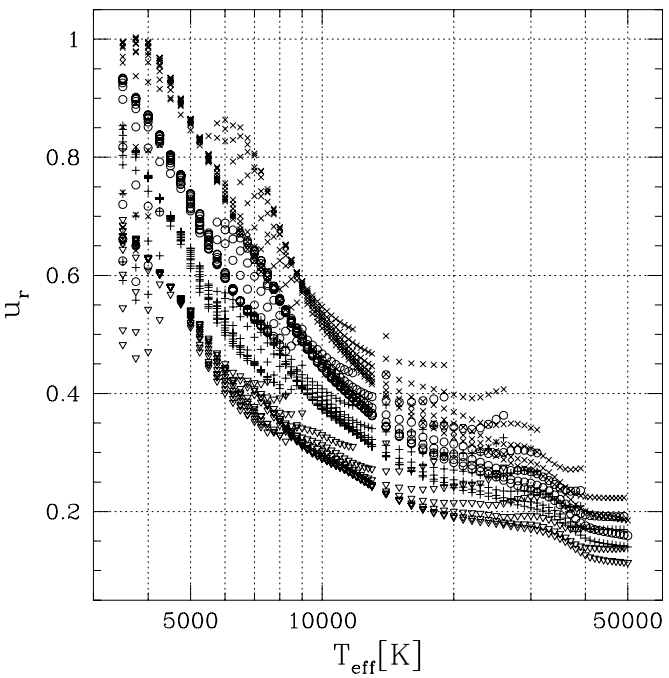

Fig. 2.—Linear limb-darkening coefficient u_r of solar abundance, $v_t = 2$ km s^{-1} Kurucz model atmospheres (Kurucz 1994), plotted as a function of effective temperature for the bands *B* (*crosses*), *V* (*circles*), *R* (*plus signs*), and *I* (*triangles*).

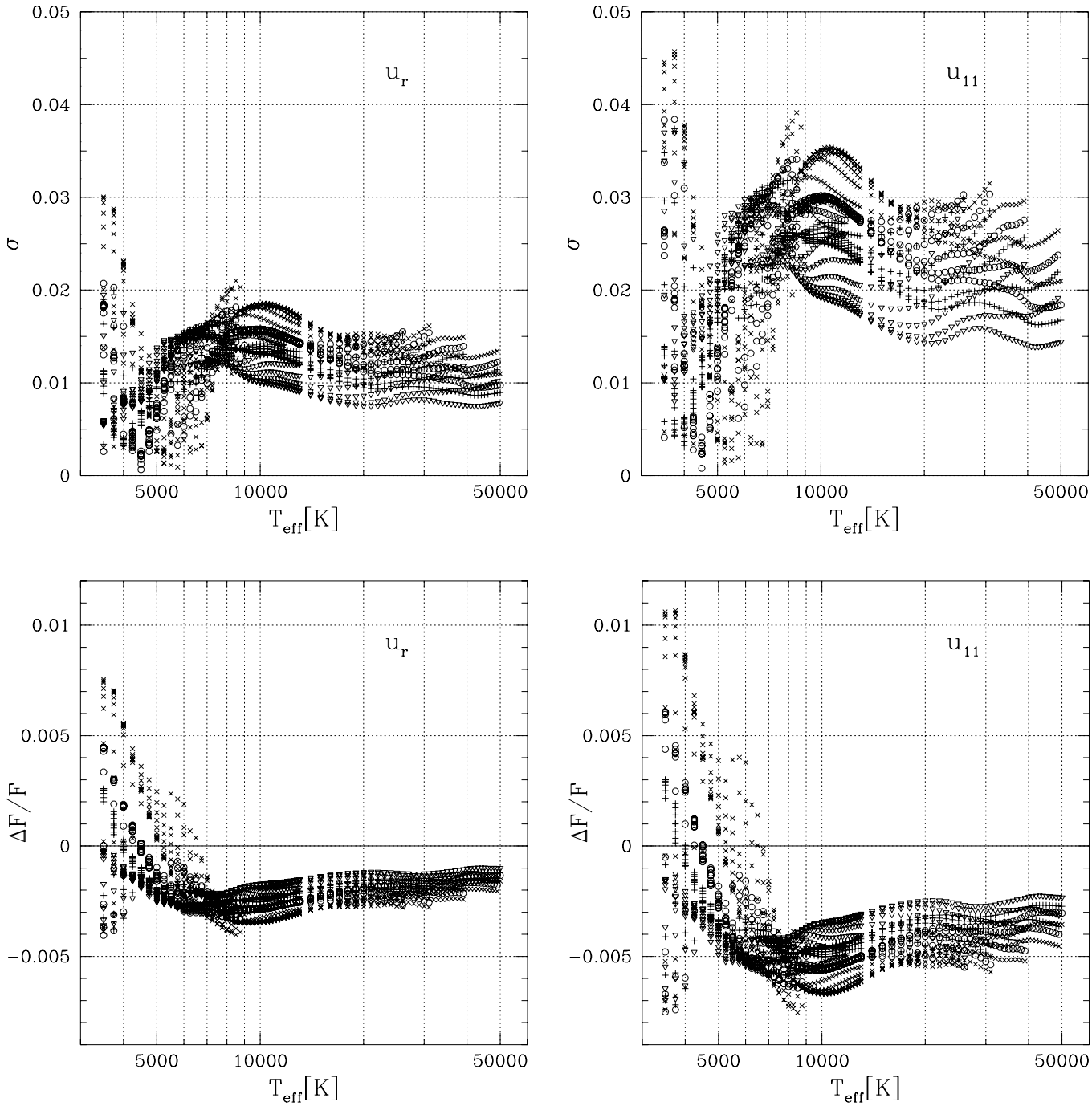

FIG. 3.—Relative rms residuals σ and relative flux excesses $\Delta F/F$ for the r-integrated limb-darkening fits from Fig. 2 (*left*) and for 11-point fits (*right*), plotted as a function of effective temperature. The range of model atmospheres and the symbols for photometric bands are the same as in Fig. 2.

reason for the excellent flux conservation[2] in μ-integration is the similar weighting of the intensity in the flux integral, as seen in equation (8). The factor r gives zero weight at the disk center and the highest (although not divergent) weight at the limb. Nevertheless, in view of the roughly 2 times higher average residual in comparison with r-integration for the four simpler limb-darkening laws, we conclude that this method suffers from a similar problem as the non–least squares flux-conservation methods (Wade & Rucinski 1985; Van Hamme 1993); that is, achieving good flux conservation at the cost of a poor fit of the intensity profile shape.

[2] Note that accuracy better than $\sim 10^{-4}$ exceeds the flux accuracy of the underlying model atmosphere data, as shown in § 5.

The obtained results support the use of r-integration fitting of the spline-interpolated intensity profile as the method of choice for computing limb-darkening coefficients.

We note that Table 1 can be also used, for example, to compare the overall quality of the limb-darkening laws for the different fitting methods. However, discussions of the different analytical laws are beyond the scope of this paper.

The main result of this section for practical purposes is the numerical difference between the limb-darkening coefficients produced by different fitting methods. We limit ourselves here to comparing those obtained by our suggested method of r-integration (hereafter u_r) with those obtained by the 11-point fit (hereafter u_{11}), the most frequently used coefficients (e.g., Díaz-Cordovés

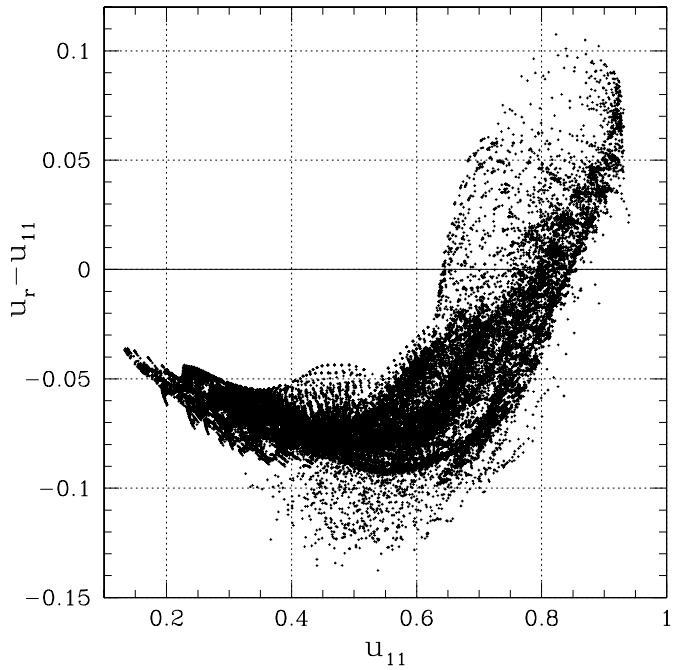

FIG. 4.—Difference between linear limb-darkening coefficients u_r and u_{11}, plotted as a function of u_{11}, for the full range of models (see text for details).

et al. 1995; Claret et al. 1995; Claret 2000). For illustration, we plot *BVRI* values of u_r in Figure 2 as a function of $T_{\rm eff}$. In order to avoid crowding, we include only solar abundance models with $v_t = 2$ km s^{-1}. The specific range of log g of the models depends on $T_{\rm eff}$. The main tendencies are well known: overall, the coefficient decreases with increasing temperature and increasing wavelength. The rms residuals and flux excesses for these models and both types of fitting are shown in Figure 3 as a function of $T_{\rm eff}$. The r-integrated fits have lower residuals and better flux conservation, in agreement with the results in Table 1.

Figure 4 illustrates the difference between u_r and u_{11} for the full range of model atmospheres, plotted as a function of u_{11}. The coefficient difference is substantial, ranging from -0.14 to 0.11 with most of the u_r being lower than u_{11}, corresponding to flatter limb-darkening profiles. At the same time, the most limb-darkened profiles are even more limb-darkened when using u_r. The results are plotted again in Figure 5 as a function of $T_{\rm eff}$ for each photometric band separately. The greatest variation occurs for lower temperature models ($T_{\rm eff} \lesssim 7000$ K) and is much reduced for higher temperature models ($T_{\rm eff} \gtrsim 10{,}000$ K). The range of coefficient differences decreases from the *B* band to the *I* band. We note specifically that 11-point fitting overestimates the limb-darkening coefficient in the *I* band for all computed models, in the *R* band for all models with $T_{\rm eff} > 4500$ K, in the *V* band for all models with $T_{\rm eff} > 6000$ K, and in the *B* band for all models with $T_{\rm eff} > 7000$ K. At lower temperatures, coefficients are overestimated for some profiles and underestimated for others.

A comparison of individual coefficients of higher order limb-darkening laws reveals that there can be even greater differences between the values obtained by different fitting methods. Nevertheless, as seen from Table 1, at the same time the overall fit quality is better, and thus the obtained combinations of coefficients produce more similar limb-darkening shapes.

4. COMPARISON WITH OBSERVATIONAL RESULTS

Following the discussions of relative merits of different limb-darkening law fitting methods, we turn to the question of observational relevance. We note that the differences between the linear coefficients demonstrated in the previous section are large enough to be detectable not only in solar limb-darkening measurements, but also, for example, in observations of caustic-crossing microlensing events or eclipsing binaries. In Cassan et al. (2006) we showed that the coefficients measured in caustic-crossing microlensing events involving K giants in the Galactic bulge are in better agreement with the values obtained by r-integration than with the 11-point fit values of Claret (2000). Here we present a comparison of these coefficients using solar limb-darkening measurements and eclipsing binary results.

4.1. *Solar Limb Darkening*

For our comparison we use measured solar limb-darkening data from Cox (2000, p. 356) for the four best-sampled wavelengths in the optical range: 450, 500, 550, and 600 nm. We compare these limb-darkening profiles with linear limb-darkening fits for the same wavelengths of the Kurucz (1994) solar model with $T_{\rm eff} = 5777$ K, $\log g = 4.4377$, [Fe/H] = 0.0, and $v_t = 1.5$ km s^{-1}. The r-integrated and 11-point fits give us coefficients u_r and u_{11}, respectively. We take these fixed coefficients and fit only the central intensity I_0 from equation (1) to get a best fit to the spline-interpolated solar limb darkening.

The relative residuals of these fits are plotted in Figure 6 for each of the wavelengths as a function of r. The values of the relative rms residual σ and relative flux excess $\Delta F/F$ are given in each of the panels. We see that for all four wavelengths u_r gives better results than u_{11}: its σ is lower by a factor of 1.3–1.7, and $\Delta F/F$ is lower by a factor of 5–21. In all cases u_{11} yields a much steeper limb-darkening profile than u_r and the measured profile. We conclude that the theoretical limb-darkening coefficient obtained by r-integrated fitting of the model atmosphere data is in substantially better agreement with the measured solar limb darkening than the coefficient obtained by 11-point fitting.

4.2. *Limb Darkening from Eclipsing Binary Analyses*

Obtaining limb-darkening coefficients from the analysis of eclipsing binary light curves is no simple task. Already Popper (1984) estimated that getting a limb-darkening coefficient with a precision of 0.1 or better requires at least 100 light-curve points within minima with a 0.005 mag photometric accuracy. Not surprisingly, there are only a few eclipsing binary systems for which limb-darkening coefficients have been extracted and published. These limb-darkening measurements have been obtained by different teams using different methods, approximations, and approaches, and are therefore also burdened by different problems. In this section we do not reanalyze any of the binary light curves. We merely perform the simplest test for our purposes, collating the published values and checking their agreement with theoretical coefficients obtained from model atmospheres as described above.

More specifically, we searched the literature for eclipsing binaries with measured limb-darkening coefficients for which estimates of $T_{\rm eff}$, log g, and [Fe/H] were also available (we note here that these estimates may sometimes also be problematic). In a number of these binaries, the coefficients for the primary and secondary stars were not measured independently. Instead, their difference was kept fixed at a value expected from some specific model atmosphere coefficients. We restrict our sample to the systems analyzed without this constraint, plus those for which the fixed difference values agree within 0.01 with those expected from our u_r coefficients *as well as* the Claret (2000) coefficients (hereafter $u_{\rm C}$). The measured *BVR* linear limb-darkening coefficients for these nine binaries are listed in Table 2 together

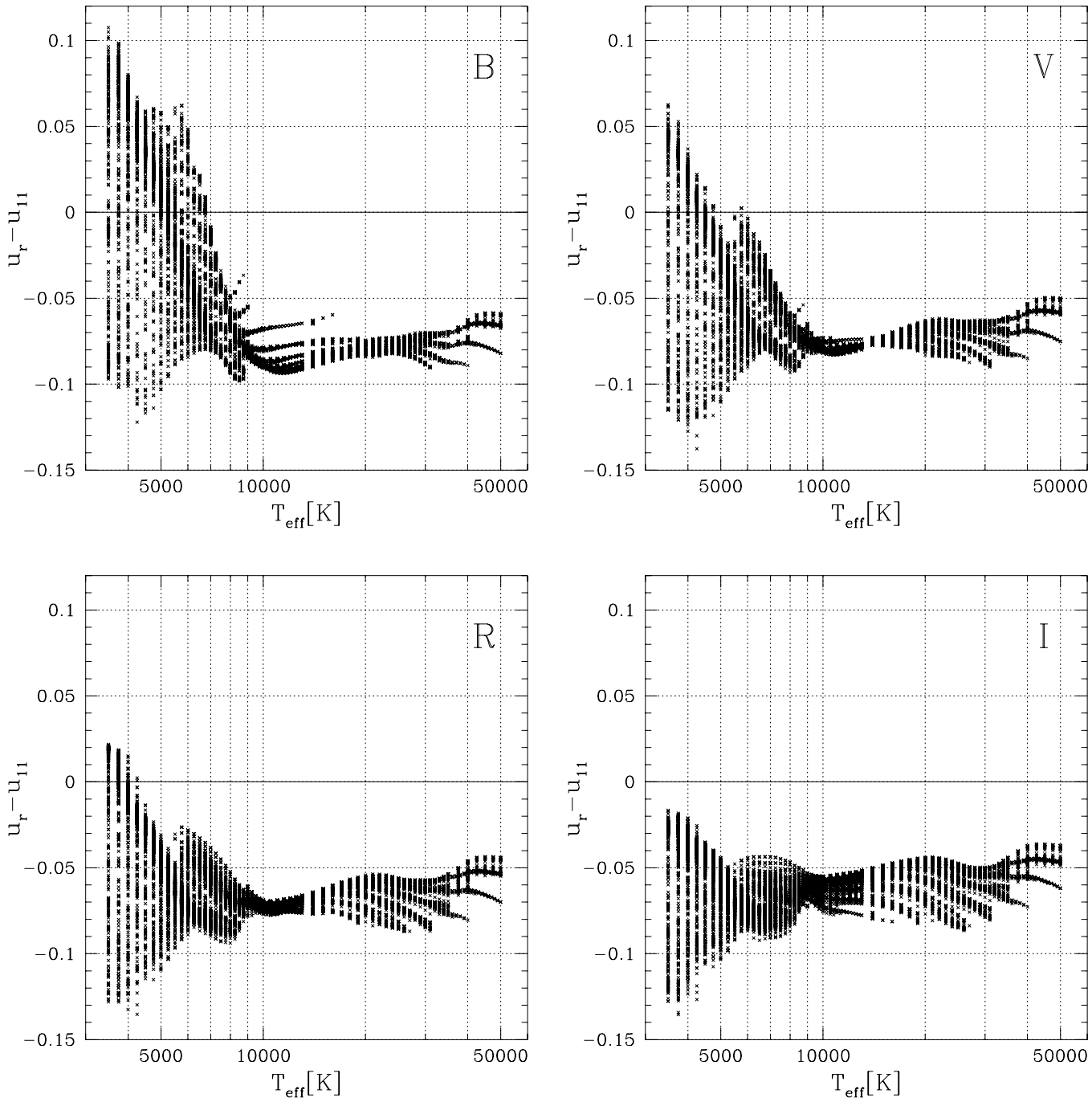

FIG. 5.—Difference between linear limb-darkening coefficients u_r and u_{11} for the full range of models, plotted separately as a function of $T_{\rm eff}$ for the bands B (*top left*), V (*top right*), R (*bottom left*), and I (*bottom right*).

with the corresponding values of u_C and u_r. These were obtained by trilinear interpolation of the values from Claret (2000) and of the values computed for the Kurucz ATLAS9 model atmosphere grid (Kurucz 1993a, 1993b, 1993c) by r-integration fitting, respectively, using the observed stars' $T_{\rm eff}$, log g, and [Fe/H] values.

For five of the binaries (BS Dra, WW Cam, V459 Cas, WW Aur, and RW Lac), all measured coefficients are closer to the u_r values, for MU Cas they are closer to the u_C values, and for the remaining three (EE Peg, FS Mon, and GG Ori), some are closer to u_r and others to u_C. Looking at the latter four systems, in the case of MU Cas we note that Lacy et al. (2004b) first obtained $u = 0.32$ for both components in an unconstrained fit, a value in perfect agreement with u_r. The value quoted in the table was obtained by fitting while keeping a fixed luminosity ratio. Turning to EE Peg (Lacy & Popper 1984), we see that the u_r values for both components are also in agreement with the measurements. The FS Mon coefficients (Lacy et al. 2000) have no error bars,[3] and the agreement with u_r in the V band is only marginally worse than that with u_C, while the agreement with u_C in the B band is substantially worse than that with u_r. In the last system, GG Ori (Torres et al. 2000), the B and R values agree better with u_r, while the V coefficients agree better with u_C. Here the situation is similar to that for MU Cas: the original unconstrained fits from two data sets produced V-band coefficients of 0.48 ± 0.08 and 0.41 ± 0.05, which are values more consistent with $u_r = 0.45$ than with $u_C = 0.51$. The unconstrained R-band value of 0.33 ± 0.13 is also in

[3] This is also the case with RW Lac.

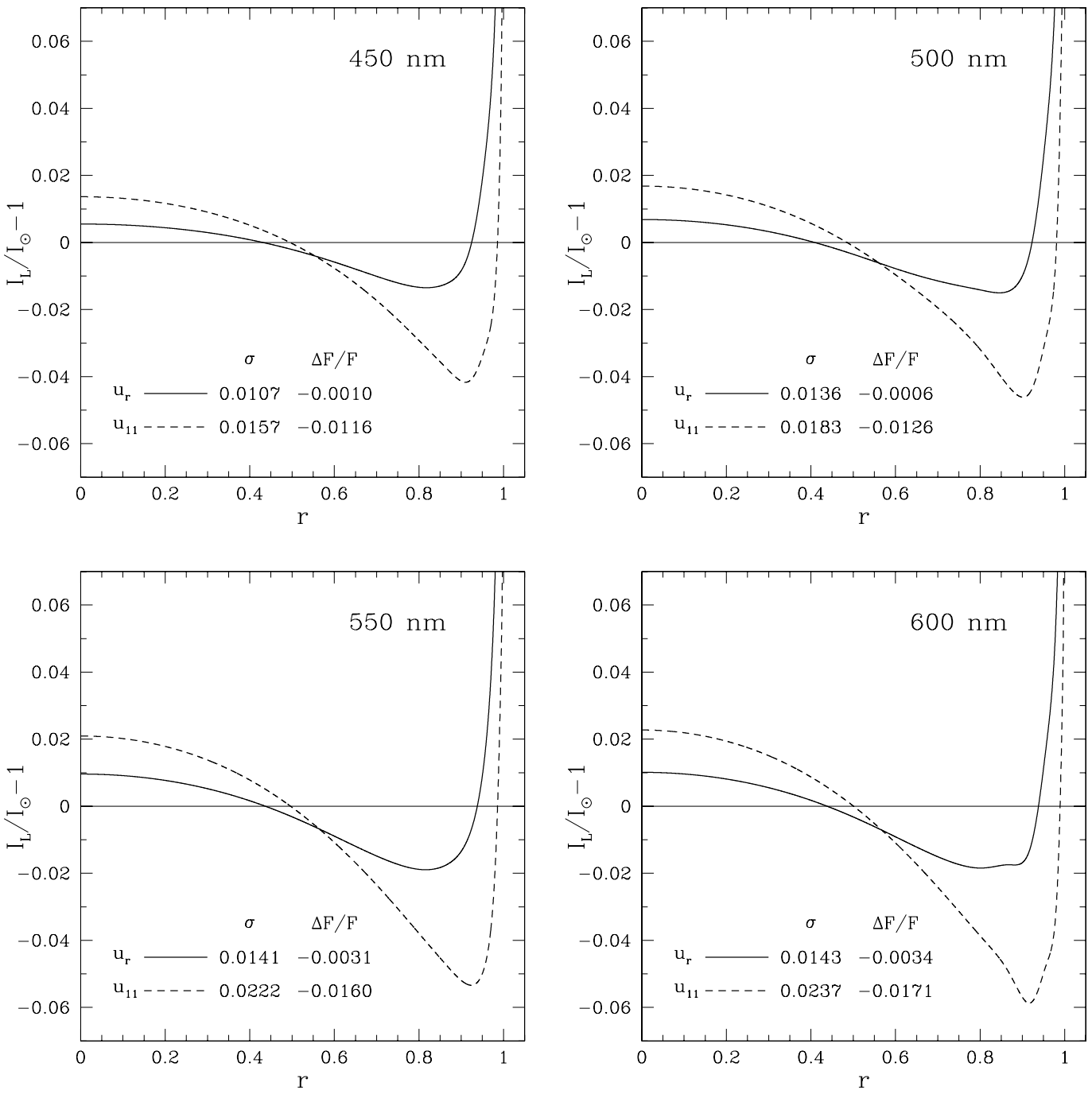

FIG. 6.—Relative residual $I_L/I_\odot - 1$ of the linear limb-darkening law I_L with theoretical coefficients u_r (*solid line*) and u_{11} (*dashed line*), compared with solar limb darkening $I_\odot$ (Cox 2000) for four wavelengths (marked in upper right corners of panels), plotted as a function of radial position r. Relative rms residuals σ and relative flux excesses $\Delta F/F$ for both fits are given in each panel.

much better agreement with $u_r = 0.38$ than the value quoted in the table.

The limb darkening of eclipsing binaries in which the radii of the components are a sufficiently large fraction of the orbital radius (>10%–15%) may be influenced by the reflection effect. In such systems the measured limb-darkening coefficient may not agree with the value given by the star's $T_{\rm eff}$. In order to avoid this potential effect, we check the results for the binaries in our selection with the smallest radii. These are RW Lac, V459 Cas, and GG Ori, with radii in the range 4%–7%. From the values in Table 2 and the discussion of GG Ori above, we see that the conclusions about the comparison of the two coefficients remain valid.

Just as in the case of caustic-crossing microlensing events, our conclusion is that for eclipsing binaries, limb-darkening coefficients obtained by our suggested method give overall better results than the widely used Claret (2000) coefficients. The systems in which the original unconstrained fits give better agreement with expected values than the photometrically adjusted fits indicate possible problems caused by poor flux conservation or, more generally, the inadequacy of the linear limb-darkening law.

5. DISCUSSION

When comparing the fitting methods in § 3, one could also evaluate the relative μ-integrated rms residual, which differs from σ in

TABLE 2
Linear Limb-darkening Coefficients Measured in Eclipsing Binaries

Binary		Measured u			Model u_C			Model u_r			Ref.
		B	V	R	B	V	R	B	V	R	
BS Dra	A	0.64 ± 0.04	0.50 ± 0.03	...	0.707	0.605	...	0.651*	0.539*	...	1
	B	0.64 ± 0.04	0.50 ± 0.03	...	0.706	0.605	...	0.650*	0.539*	...	
EE Peg	A	0.62 ± 0.03	...	...	0.660	...	...	0.597*	...	...	2
	B	0.75 ± 0.15	...	...	0.740*	...	...	0.689	...	...	
FS Mon	A	0.58	0.58	...	0.710	0.607*	...	0.654*	0.540	...	3
	B	0.594	0.591	...	0.718	0.614*	...	0.664*	0.548	...	
GG Ori	A	0.50 ± 0.04	0.51 ± 0.03	0.23 ± 0.07	0.594	0.513*	0.432	0.521*	0.446	0.377*	4
	B	0.50 ± 0.04	0.51 ± 0.03	0.23 ± 0.07	0.594	0.513*	0.432	0.521*	0.446	0.377*	
WW Cam	A	...	0.494 ± 0.017	...	...	0.601	...	...	0.533*	...	5
	B	...	0.499 ± 0.017	...	...	0.606	...	...	0.538*	...	
V459 Cas	A	...	0.487 ± 0.008	...	...	0.546	...	...	0.479*	...	6
	B	...	0.487 ± 0.008	...	...	0.548	...	...	0.481*	...	
MU Cas	A	...	0.56 ± 0.07	...	...	0.392*	...	...	0.331	...	7
	B	...	0.56 ± 0.07	...	...	0.399*	...	...	0.337	...	
WW Aur	A	0.616 ± 0.056	0.416 ± 0.060	...	0.692	0.598	...	0.625*	0.528*	...	8
	B	0.512 ± 0.078	0.418 ± 0.083	...	0.688	0.593	...	0.618*	0.518*	...	
RW Lac	A	...	0.55	...	...	0.668	...	...	0.611*	...	9
	B	...	0.57	...	...	0.689	...	...	0.638*	...	

Notes.—For each eclipsing binary, the primary star is marked by A and the secondary by B. Model coefficients are based on Kurucz ATLAS9 atmospheres: u_C is taken from Claret (2000), and u_r is computed in this work. The better agreeing coefficient is marked with an asterisk (*).

References.—(1) Popper & Etzel 1981; (2) Lacy & Popper 1984; (3) Lacy et al. 2000; (4) Torres et al. 2000; (5) Lacy et al. 2002; (6) Lacy et al. 2004a; (7) Lacy et al. 2004b; (8) Southworth et al. 2005; (9) Lacy et al. 2005.

equation (7) by using Δ_μ in the numerator and integrating over μ instead of r in the denominator. Such a residual is by definition lowest for the results obtained by μ-integration. For the linear law, we get an average residual of 3.28% and maximum residual of 6.94%, both of which are higher than the corresponding r-integrated residuals. We get similar results even for the second-order laws. This only demonstrates that fitting of simple analytical laws is more difficult in terms of μ than in terms of r. As noted before, fitting by integration over μ gives very high weight to the limb, where attempts to fit the more complex intensity dependence reduce the quality of the remaining fit. Only the five-term law of Claret (2000) has an average μ-integrated residual lower than its average r-integrated residual, even though its maximum μ-integrated residual remains higher. This law therefore tends to fit the limb darkening close to the limb slightly better than closer to the center.

In this work we interpolated intensity data points using cubic spline interpolation in terms of μ with natural boundary conditions; that is, zero second derivative at $\mu = 0$ and $\mu = 1$. In order to check the sensitivity of the results to the interpolation method, we tested using cubic spline interpolation in terms of r with zero first derivative at the center and zero second derivative at the limb. We note that this interpolation is not esthetically optimal, as in the region closest to the limb the r dependence is very steep, so that it can produce small wiggles in the spline at the limb, which are noticeable when the spline is plotted as a function of μ. Still, the obtained linear coefficients differ at most in the third decimal place.

Similarly, we tested the influence of different boundary conditions for the μ spline. Changing the boundary condition at the limb or the method of extrapolating the limb intensity had a negligible influence, on the order of 10^{-7} in flux or less. Changing the boundary condition at the center to equality of the first and second derivatives (which gives an interpolation equally pleasing to the eye) had a larger influence, although still only on the order of 10^{-4} in flux or less. The difference is due to the larger spacing of model atmosphere rays at the center. On the basis of this test, we can consider the value of 10^{-4} as a limiting flux accuracy for the model atmosphere data used in this work.

6. SUMMARY AND CONCLUSIONS

We have studied the sensitivity of limb-darkening coefficients computed from stellar atmosphere models to different least-squares fitting methods. Tests with Kurucz ATLAS9 model atmospheres (Kurucz 1993a, 1993b, 1993c, 1994) show that best results are obtained by suitably interpolating the available intensity points and fitting limb-darkening laws to the obtained intensity profile $\tilde{I}$ by minimizing the r-integrated squared residual introduced in equation (5). Other methods give too much weight to the quality of the fit in a narrow region at the stellar limb.

The differences between the coefficient values computed by the different methods are substantial. In particular, we have shown that linear limb-darkening coefficients of *BVRI* profiles of Kurucz models computed by the suggested method differ by as much as 0.14 from values obtained by a commonly used fitting method with points roughly evenly spaced in terms of μ. Such differences are observationally significant. The plots in Figure 6 illustrate that coefficients computed from a solar model atmosphere by the preferred fitting are in better agreement with solar limb-darkening data. In Table 2 we have further demonstrated that available limb-darkening measurements from eclipsing binaries are more compatible with the newly computed coefficients than with those from Claret (2000). We have previously reached a similar conclusion with limb-darkening measurements from caustic-crossing gravitational microlensing events (Cassan et al. 2006).

Other methods of measuring limb darkening, such as stellar interferometry or observation of extrasolar planet transits, can use a similar approach when comparing measured coefficients with theoretical predictions. However, all these methods may run into problems with analytical limb-darkening laws. The limb-darkening signature in the data is usually not strong enough for a reliable extraction of more than a single limb-darkening

coefficient; that is, the linear coefficient. At the same time, even at the photometric accuracy of the available data, the linear law is in many cases an inadequate approximation, largely due to its poor flux conservation and generally poor matching of the limb-darkening shape.

The drawbacks of measuring coefficients of analytical laws can be bypassed by using an alternative description of limb darkening, obtained by principal component analysis of an ensemble of model atmosphere intensity profiles (Heyrovský 2003). At the cost of not being analytical, such an approach gives the best possible limb-darkening description as a linear combination of the least number of terms. The principal component description is therefore also ideally suited for measuring stellar limb darkening, as demonstrated by Heyrovský (2003) in the case of microlensing events.

It is a pleasure to thank Jean-Philippe Beaulieu for his hospitality at the Institut d'Astrophysique de Paris. This work was supported by the Czech Science Foundation grant GACR 205/04/P256.

REFERENCES

Barban, C., Goupil, M. J., Van't Veer-Menneret, C., Garrido, R., Kupka, F., & Heiter, U. 2003, A&A, 405, 1095
Bessell, M. S. 1990, PASP, 102, 1181
Cassan, A., et al. 2006, A&A, 460, 277
Claret, A. 2000, A&A, 363, 1081
Claret, A., Díaz-Cordovés, J., & Giménez, A. 1995, A&AS, 114, 247
Claret, A., & Giménez, A. 1990, A&A, 230, 412
Cox, A. N., ed. 2000, Allen's Astrophysical Quantities (4th ed.; New York: AIP)
Deeg, H. J., Garrido, R., & Claret, A. 2001, NewA, 6, 51
Díaz-Cordovés, J., Claret, A., & Giménez, A. 1995, A&AS, 110, 329
Heyrovský, D. 2003, ApJ, 594, 464
Kurucz, R. L. 1993a, Kurucz CD-ROM 13, ATLAS9 Stellar Atmosphere Programs and 2 km/s Grid (Cambridge: SAO)
———. 1993b, Kurucz CD-ROM 16, Limbdarkening for 2 km/s Grid (No. 13): [+1.0] to [−1.0] (Cambridge: SAO)
———. 1993c, Kurucz CD-ROM 17, Limbdarkening for 2 km/s Grid (No. 13): [+0.0] to [−5.0] (Cambridge: SAO)
———. 1994, Kurucz CD-ROM 19, Solar Abundance Model Atmospheres for 0, 1, 2, 4, 8 km/s (Cambridge: SAO)
Lacy, C. H., & Popper, D. M. 1984, ApJ, 281, 268
Lacy, C. H. S., Claret, A., & Sabby, J. A. 2004a, AJ, 128, 1340
———. 2004b, AJ, 128, 1840
Lacy, C. H. S., Torres, G., Claret, A., & Sabby, J. A. 2002, AJ, 123, 1013
Lacy, C. H. S., Torres, G., Claret, A., Stefanik, R. P., Latham, D. W., & Sabby, J. A. 2000, AJ, 119, 1389
Lacy, C. H. S., Torres, G., Claret, A., & Vaz, L. P. R. 2005, AJ, 130, 2838
Manduca, A., Bell, R. A., & Gustafsson, B. 1977, A&A, 61, 809
Popper, D. M. 1984, AJ, 89, 132
Popper, D. M., & Etzel, P. B. 1981, AJ, 86, 102
Quirrenbach, A., Mozurkewich, D., Buscher, D. F., Hummel, C. A., & Armstrong, J. T. 1996, A&A, 312, 160
Southworth, J., Smalley, B., Maxted, P. F. L., Claret, A., & Etzel, P. B. 2005, MNRAS, 363, 529
Torres, G., Lacy, C. H. S., Claret, A., & Sabby, J. A. 2000, AJ, 120, 3226
Van Hamme, W. 1993, AJ, 106, 2096
Wade, R. A., & Rucinski, S. M. 1985, A&AS, 60, 471
Witt, H. J. 1995, ApJ, 449, 42